

Contribution from the Department of Chemistry, University of British Columbia, Vancouver, BC, Canada V6T 1Y6, and Department of Physics, National Research Centre "Demokritos", Paraskevi, Attiki, Greece

Low-Dimensional Magnetic Exchange in the Pyrazine-Bridged Complexes $\text{Fe}(\text{pyz})_2(\text{NCS})_2$ and $\text{Fe}(\text{pyz})(\text{NCO})_2$

J. S. Haynes,[†] A. Kostikas,[‡] J. R. Sams,^{*††} A. Simopoulos,[†] and R. C. Thompson^{*†}

Received November 3, 1986

The title compounds have been prepared and characterized by electronic, vibrational, and Mössbauer spectroscopies and by magnetic susceptibility measurements. Spectroscopic data indicate that $\text{Fe}(\text{pyz})_2(\text{NCS})_2$ adopts a 2D pyrazine-bridged lattice with N-bonded monodentate NCS^- ions in axial positions. Mössbauer spectra show the onset of magnetic hyperfine splitting at a temperature of 9.1 ± 0.2 K, and there is a maximum in the susceptibility at ~ 8 K, indicating a transition to an antiferromagnetically ordered state. The electric field gradient (EFG) is axial, and the electronic ground state is $^5\text{B}_{2g}$, corresponding to an axial compression of the $\text{FeN}_4\text{N}'_2$ octahedron. The hf field of 27.7 T (at 1.80 K) is canted at an angle $\theta = 41^\circ$ with respect to V_{zz} , the z component of the EFG, and the angle ϕ is indeterminate due to the axial symmetry. $\text{Fe}(\text{pyz})(\text{NCO})_2$ contains bidentate bridging $>\text{NCO}^-$ ions forming linear chains, which are cross-linked by symmetrically bridging pyrazine ligands. This complex shows a broad susceptibility maximum at ~ 38 K, and Mössbauer spectroscopy indicates $T_N = 27.05 \pm 0.05$ K, with the coexistence of a superparamagnetic component persisting to $T/T_N = 0.83$. The magnetic structure is that of a 2D Ising system, with the hf field (18.0 T at 4.2 K) parallel to V_{yy} , which is assumed to be the linear chain direction. In the range $0.8 \leq T/T_N \leq 0.98$ the critical exponent $\beta = 0.12$, in agreement with the theoretical value $\beta = 1/8$ for the 2D Ising model.

Introduction

The ability of 1,4-diazine (pyrazine, pyz) to bridge transition-metal ions so as to form one-dimensional linear chains or two-dimensional layer compounds is well documented.¹⁻³ Such inorganic coordination polymers are of interest both because of their low-dimensional characteristics^{4,5} and because of the capability of pyrazine to support magnetic superexchange between the metal centers.

The most extensively studied complexes of this type have been copper(II) derivatives,⁶⁻¹¹ where it has been found that an important factor in determining the nature of the exchange interactions is the overlap between the copper d orbitals and the pyrazine π system.^{2,11-13} Effective overlap depends on the degree of tilting of the pyrazine ring with respect to the xy coordination plane. For example, in $\text{Cu}(\text{pyz})(\text{NO}_3)_2$ this angle is 48° and orbital overlap between the pyrazine π system and the copper $|x^2 - y^2\rangle$ ground state results in an effective route for magnetic exchange. However, in $\text{Cu}(\text{pyz})(\text{hfac})_2$ ($\text{hfac} = \text{hexafluoro-pentane-1,4-dionate}$),¹² a linear-chain structure results from pyrazine bridging between the square-planar $\text{Cu}(\text{hfac})_2$ units, with pyrazine coordinating along the z direction. There is no effective $d-\pi$ overlap, and no exchange interactions are observed.¹³

A particularly interesting example that appears to incorporate both of these features is the recently reported¹¹ $\text{Cu}(\text{pyz})_2(\text{CH}_3\text{SO}_3)_2$. The structure is made up of parallel sheets, each consisting of a square array of copper(II) ions bridged by two types of bidentate pyrazine ligands. The equatorial plane around each copper ion contains two pyrazine nitrogen atoms ($\text{Cu}-\text{N}(1) = 2.058 \text{ \AA}$) and two oxygen atoms from monodentate methanesulfonate groups ($\text{Cu}-\text{O} = 1.956 \text{ \AA}$); the axial coordination sites are occupied by bridging pyrazine groups with substantially longer $\text{Cu}-\text{N}$ bond lengths ($\text{Cu}-\text{N}(2) = 2.692 \text{ \AA}$). The equatorial pyrazine rings are canted at an angle of 28.5° to the xy plane, while the axially bound pyrazine rings lie in the xz plane where there is no effective $d-\pi$ overlap. The complex shows antiferromagnetic behavior with a susceptibility maximum at about 6.2 K, and the exchange coupling is probably best described in terms of a linear chain involving the equatorial pyrazine ligands.

The magnetic properties of several other transition-metal-pyrazine complexes have also been investigated. For example, the cobalt(II) pyrazine halides $\text{Co}(\text{pyz})_2\text{X}_2$ ($\text{X} = \text{Cl}, \text{Br}$) gave no evidence of magnetic exchange down to 1.8 K,¹⁴ although at lower temperatures both complexes order antiferromagnetically,^{15,16} with Néel points of 0.85 and 0.66 K, respectively. The nickel(II) derivatives $\text{Ni}(\text{pyz})_2\text{X}_2$ ($\text{X} = \text{Cl}, \text{Br}, \text{I}$)¹⁷ showed temperature-independent magnetic moments between 300 and 90 K, but they

do not appear to have been studied at lower temperatures. Evidence for magnetic exchange has been found in the silver(II) complex $\text{Ag}(\text{pyz})_2\text{S}_2\text{O}_8$, where the moment is only $1.27 \mu_B$ at 80 K.¹⁸

We have reported very recently spectroscopic and magnetic measurements on the iron(II) bis(pyrazine) halides $\text{Fe}(\text{pyz})_2\text{X}_2$ ($\text{X} = \text{Cl}, \text{Br}, \text{I}$) and the mono(pyrazine) complex $\text{Fe}(\text{pyz})\text{Cl}_2$,¹⁹ some of which had been studied previously.²⁰⁻²³ Similar but less extensive measurements on the bis(pyrazine) derivatives have been reported independently by Rachlewicz et al.²⁴ From susceptibility measurements between 300 and 4.2 K [and to 1.9 K for $\text{Fe}(\text{pyz})\text{Cl}_2$], we could find no conclusive evidence for exchange coupling in these complexes. The Mössbauer spectra of Reiff and co-workers²⁵ show that both $\text{Fe}(\text{pyz})_2\text{Cl}_2$ and $\text{Fe}(\text{pyz})\text{Cl}_2$ are

- Carreck, P. W.; Goldstein, M.; McPartlin, E. M.; Unsworth, W. D. *J. Chem. Soc., Chem. Commun.* **1971**, 1634.
- Santoro, A.; Mighell, A. D.; Reimann, C. W. *Acta Crystallogr., Sect. B: Struct. Crystallogr. Cryst. Chem.* **1970**, *B26*, 979.
- Darriet, J.; Haddad, M. S.; Duesler, E. N.; Hendrickson, D. N. *Inorg. Chem.* **1979**, *18*, 2679.
- Miller, J. S.; Epstein, A. J., Eds. *Ann. N.Y. Acad. Sci.* **1978**, 313.
- Alcacer, L., Ed. *The Physics and Chemistry of Low-Dimensional Solids*; Reidel: Dordrecht, 1980.
- Inman, G. W.; Hatfield, W. E. *Inorg. Chem.* **1972**, *11*, 3085.
- Villa, J. F.; Hatfield, W. E. *J. Am. Chem. Soc.* **1971**, *93*, 4081.
- Boyd, P. D. W.; Mitra, S. *Inorg. Chem.* **1980**, *19*, 3547.
- Richardson, H. W.; Hatfield, W. E. *J. Am. Chem. Soc.* **1976**, *98*, 835.
- Haddad, M. S.; Hendrickson, D. N.; Canady, J. P.; Drago, R. S.; Biekza, D. S. *J. Am. Chem. Soc.* **1979**, *101*, 898.
- Haynes, J. S.; Rettig, S. J.; Sams, J. R.; Thompson, R. C.; Trotter, J. *Can. J. Chem.* **1987**, *65*, 420.
- Belford, R. C. E.; Fenton, D. E.; Truter, M. R. *J. Chem. Soc., Dalton Trans.* **1974**, 17.
- Richardson, H. W.; Wasson, J. R.; Hatfield, W. E. *Inorg. Chem.* **1977**, *16*, 484.
- Inoue, M.; Kubo, M. *Coord. Chem. Rev.* **1976**, *21*, 1.
- Gonzalez, D.; Bartolomé, J.; Navarro, R.; Greidanus, F.; de Jongh, L. *J. Phys. Colloq.* **1978**, *39*, 762.
- Carlin, R. L.; Carnegie, D. W.; Bartolomé, J.; Gonzalez, D.; Floria, L. *M. Phys. Rev. B* **1985**, *32*, 7476.
- Goldstein, M.; Taylor, F. B.; Unsworth, W. D. *J. Chem. Soc., Dalton Trans.* **1972**, 418.
- Matthews, R. W.; Walton, R. A. *Inorg. Chem.* **1971**, *10*, 1433.
- Haynes, J. S.; Sams, J. R.; Thompson, R. C. *Inorg. Chem.* **1986**, *25*, 3740.
- Child, M. D.; Foulds, G. A.; Percy, G. C.; Thornton, D. A. *J. Mol. Struct.* **1981**, *75*, 191.
- Beech, G.; Mortimer, C. T. *J. Chem. Soc. A* **1967**, 1115.
- Ferraro, J. R.; Zipper, J.; Wozniak, W. *Appl. Spectrosc.* **1969**, *23*, 160.
- Bayer, R.; Ferraro, J. R. *Inorg. Chem.* **1969**, *8*, 1654.
- Rachlewicz, K.; Pietrzyk, J.; Drabent, K. *Polyhedron* **1985**, *4*, 1777.

[†] University of British Columbia.

[‡] National Research Centre "Demokritos".

Table I. Pyrazine Vibrational Bands in the Free Ligand and Iron(II) Complexes^a

compd	infrared freq, cm ⁻¹							
pyrazine ^b	3066 w	1490 s	1178 m	1067 vs	926 vw	823 vw	789 w	597 w
	2973 w	1418 vs	1148 vs	1048 vw		804 vs	752 vw	417 m
			1125 w	1032 vw				700 vw
			1110 m	1022 m				
				1006 w				
Fe(py ₂) ₂ (NCS) ₂	3110 m	1489 m	1161 s	1083 w	982 w		779 s	461 s
	3090 m	1415 s	1125 s	1051 s	972 w		790 s	
	3040 m		1112 m		970 sh			
Fe(py ₂)(NCO) ₂	3100 m	1487 m	1171 m	1062 s			798 s	467 s
		1416 s	1120 s					

^a Abbreviations: s, strong; m, medium; w, weak; v, very; sh, shoulder. ^b From ref 34.

fast-relaxing paramagnets in zero field down to 0.52 K. Below 0.5 K, however, the bis(pyrazine) complex shows relaxation broadening and hyperfine structure arising from incipient magnetic ordering, whereas the spectrum of the mono(pyrazine) derivative remains a symmetric quadrupole doublet down to 0.33 K.²⁶ The absence of any Zeeman splitting in the Mössbauer spectra of Fe(py₂)Cl₂ at the lowest temperatures studied could conceivably result either from a fortuitous cancellation of the various components that comprise the internal hyperfine field or from a substantial zero-field splitting that produces a nonmagnetic (singlet) ground state. Interestingly, both Ni(py₂)Cl₂ and Mn(py₂)Cl₂ exhibit antiferromagnetic susceptibility maxima at about 10 and 2.5 K, respectively.²⁶

We wish to report now the synthesis and characterization, by electronic, vibrational, and Mössbauer spectroscopies and magnetic susceptibility measurements, of two pyrazine-bridged pseudohalide complexes of iron(II), Fe(py₂)₂(NCS)₂ and Fe(py₂)(NCO)₂. The thiocyanato derivative was reported previously,²⁷ but the synthetic procedure was not given and the complex was incompletely characterized. Both complexes exhibit susceptibility maxima indicative of antiferromagnetic exchange, and Mössbauer spectra reveal magnetic phase transitions. A preliminary report on some of this work has recently appeared.²⁸

Experimental Section

Materials and Physical Measurements. All chemicals were at least of reagent grade quality and were obtained from commercial sources. Methanol was dried by refluxing in the presence of magnesium methoxide. Water was degassed immediately prior to use by several freeze-pump-thaw cycles. Manipulations were carried out either in a nitrogen atmosphere drybox or by using standard Schlenk techniques. Elemental analyses were performed by P. Borda of UBC.

Electronic spectra were obtained by using equipment and procedures described previously.²⁹ Infrared spectra were recorded on samples milled in Nujol sandwiched between KRS-5 plates. A Perkin-Elmer 598 spectrophotometer was used in the range 250–4000 cm⁻¹. All spectra were calibrated with use of a polystyrene film.

Magnetic susceptibility measurements between 4.2 and 130 K employed a vibrating-sample magnetometer,³⁰ and between 80 and 300 K the Gouy technique was used.²⁹ Susceptibilities at room temperature were also measured with a Faraday magnetic balance³¹ at three different values of HdH/dx . No field dependence was observed. Molar magnetic susceptibilities were corrected for the diamagnetism of the metal ion and ligands as follows (in units of 10⁻⁶ cm³ mol⁻¹): Fe²⁺, -13; C₄H₄N₂, -45; NCO⁻, -21; NCS⁻, -35.

⁵⁷Fe Mössbauer spectra were recorded in transmission mode, with constant-acceleration spectrometers of conventional design. The Doppler velocity scale was calibrated with an iron-foil absorber, and isomer shifts

are quoted relative to the centroid of the iron-foil spectrum. Spectra in the paramagnetic region were fitted by least-squares techniques to Lorentzian line shapes. In the antiferromagnetic regime, the hyperfine-split spectra were simulated by using a static molecular field model based on the method of Kündig.³²

Syntheses. **Bis(pyrazine)iron(II) Thiocyanate, Fe(py₂)₂(NCS)₂.** Iron(II) sulfate heptahydrate (0.672 g, 2.24 mmol) and potassium thiocyanate (0.470 g, 4.84 mmol) were separately dissolved in water (10 and 5 mL, respectively). The potassium thiocyanate solution was added to the iron(II) solution, and the mixture was filtered directly into a solution of pyrazine (0.535 g, 5.57 mmol) dissolved in water (10 mL). An orange-brown precipitate resulted; the solution was stirred for 0.75 h, and the product was isolated by filtration and washed with water and methanol (67% yield). Anal. Calcd for FeC₁₀H₈N₆S₂: C, 36.18; H, 2.43; N, 25.31. Found: C, 35.82; H, 2.30; N, 25.10.

(Pyrazine)iron(II) Cyanate, Fe(py₂)(NCO)₂. Iron(II) sulfate heptahydrate (1.079 g, 3.88 mmol) was dissolved in water (5 mL). To this solution was added an aqueous solution (5 mL) of potassium cyanate (0.644 g, 7.94 mmol). The resulting solution was filtered directly into an aqueous solution (10 mL) of pyrazine (0.645 g, 8.05 mmol). A dark purple solid formed instantly, and the mixture was stirred for 2 h. The product was isolated in 77% yield after filtration and washing with small quantities of water and methanol. Anal. Calcd for FeC₆H₄N₄O₂: C, 32.76; H, 1.83; N, 25.47; O, 14.55. Found: C, 32.69; H, 1.89; N, 25.31; O, 14.62.

Results and Discussion

Although essentially identical preparative routes were employed for the cyanate and thiocyanate complexes, compounds of different stoichiometries were obtained. Attempts to prepare Fe(py₂)₂(NCO)₂ using pyrazine:iron ratios substantially greater than 2:1 still resulted in isolation of the mono(pyrazine) complex.

Both of the present complexes are extremely insoluble and were obtained in the form of fine powders. Attempts to grow single crystals suitable for X-ray diffraction studies were unsuccessful, and our structural conclusions are based on spectroscopic evidence. These data, although indirect, leave little doubt concerning the correct formulation of the structures of the complexes.

Infrared Spectra. Electron diffraction studies³³ have shown the free pyrazine molecule to be planar (D_{2h} point group), and infrared assignments have been made on this basis by Lord et al.³⁴ When both nitrogen atoms of pyrazine coordinate equivalently to metal centers in a bridging mode, D_{2h} symmetry is retained; however, when only one nitrogen atom is coordinated in a unidentate fashion, the symmetry is reduced at least to C_{2v} , and vibrational bands forbidden under D_{2h} become active in the infrared spectrum. Bands assigned to the internal vibrations of the pyrazine ligand are listed in Table I, and the infrared spectra of the complexes are illustrated in Figure S1.³⁵

Upon coordination, most of the pyrazine absorption bands exhibit shifts. The most coordination-sensitive of these bands, at 417 cm⁻¹ in the uncoordinated ligand,³⁴ is shifted by 40–50 cm⁻¹ to higher frequency on complex formation. The infrared activity of the pyrazine vibrations in the present complexes is similar to that found in known pyrazine-bridged complexes^{17,36} but very

(25) Reiff, W. M.; Zhang, J. H.; Takacs, J.; Takacs, L. *Proc. Int. Conf. Appl. Mössbauer Eff.* **1985**, paper 2.04.

(26) Reiff, W. M., personal communication.

(27) Figgis, B. N.; Lewis, J.; Mabbs, F. E.; Webb, G. A. *J. Chem. Soc. A* **1967**, 442.

(28) Haynes, J. S.; Kostikas, A.; Sams, J. R.; Simopoulos, A.; Thompson, R. C. *Hyperfine Interact.* **1986**, *28*, 815.

(29) Haynes, J. S.; Sams, J. R.; Thompson, R. C. *Can. J. Chem.* **1981**, *59*, 669.

(30) Haynes, J. S.; Oliver, K. W.; Rettig, S. J.; Thompson, R. C.; Trotter, J. *Can. J. Chem.* **1984**, *62*, 891.

(31) Herring, F. G.; Landä, B.; Thompson, R. C.; Schwerdtfeger, C. F. *J. Chem. Soc. A* **1971**, 528.

(32) Kündig, W. *Nucl. Instrum. Methods* **1967**, *48*, 219.

(33) Schomaker, V.; Pauling, L. *J. Am. Chem. Soc.* **1939**, *61*, 1769.

(34) Lord, R. C.; Marston, A. L.; Miller, F. A. *Spectrochim. Acta* **1957**, *9*, 113.

(35) Supplementary material.

different from that in complexes where pyrazine bonds in a unidentate mode.³⁶ In particular, infrared spectra of the latter complexes, and the Raman spectrum of free pyrazine,³⁶ show bands at about 1230, 920, and 750 cm^{-1} , whereas the present complexes have no absorption bands in these regions. It is thus clear that the pyrazine groups in both complexes are functioning as bridging ligands between iron(II) ions, with retention of D_{2h} symmetry.

The infrared spectra also provide insight into the coordination modes of the anions in these complexes. We consider first $\text{Fe}(\text{pyz})_2(\text{NCS})_2$. Infrared criteria to determine the mode of coordination of the thiocyanate ion have been developed.³⁷⁻⁴⁰ Several possibilities exist: coordination to the metal through nitrogen only (thiocyanato-*N*), coordination through sulfur only (thiocyanato-*S*), or bridging two metal ions to form $\text{M}-\text{NCS}-\text{M}'$ units. These three types of coordination are well-known,³⁹ and other modes of bridging such as $>\text{NCS}^-$ or $>\text{SCN}^-$ are also possible.

The vibrational modes of the NCS^- ion are appreciably mixed but can be designated: ν_1 as ν_{CN} , ν_2 as δ_{NCS} , and ν_3 as ν_{CS} . The infrared spectrum of the free anion in KNCS ⁴¹ shows three bands, which have been assigned as follows (values are in cm^{-1}): ν_1 2053 s; ν_2 486 m, 471 m; ν_3 746 m. The splitting of ν_2 is attributed to a solid-state effect. The anion bands in the spectrum of $\text{Fe}(\text{pyz})_2(\text{NCS})_2$ (see Figure S1) are assigned as follows (cm^{-1}): ν_1 2060 s, 2000 sh; ν_2 493 m; ν_3 824 m. All three bands can be used to diagnose the thiocyanate coordination mode.³⁹

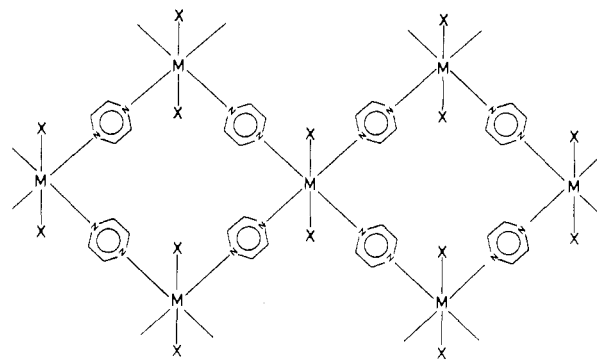
The intense C-N stretching vibration, ν_1 , at 2060 cm^{-1} is similar to the value of 2065 cm^{-1} observed in the thiocyanato-*N* complex, $\text{Fe}(\text{py})_4(\text{NCS})_2$ ⁴² (py = pyridine). It has been found³⁹ that thiocyanato-*N* coordination results in little change in the position of ν_1 from the free-ion value, while thiocyanato-*S* bonding results in a shift to approximately 2100 cm^{-1} . In bridging ($-\text{NCS}-$) thiocyanate complexes ν_1 occurs well above 2100 cm^{-1} .³⁹ The ν_1 value of 2060 cm^{-1} observed for $\text{Fe}(\text{pyz})_2(\text{NCS})_2$ is consistent with the presence of a terminally N-bonded NCS^- anion.

For ν_3 , frequencies in the 700- cm^{-1} region are taken as indicative of S-bonding, while those at approximately 800 cm^{-1} indicate N-bonding.³⁹ The infrared spectrum of $\text{Fe}(\text{pyz})_2(\text{NCS})_2$ lacks absorption bands in the 650-750- cm^{-1} region, so that S-bonding is not suspected. There are three bands near 800 cm^{-1} , two of which are assigned to pyrazine; the third band at 824 cm^{-1} is assigned to the ν_3 anion mode. This value compares favorably with that of 810 cm^{-1} found in $\text{Fe}(\text{py})_4(\text{NCS})_2$ ⁴² and further supports an N-coordination mode for the anion.

A single sharp ν_2 band in the region of 480 cm^{-1} is indicative of N-bonding, whereas the presence of several bands of low intensity near 400 cm^{-1} indicates S-bonding.³⁹ The spectrum of $\text{Fe}(\text{pyz})_2(\text{NCS})_2$ shows two sharp bands of medium intensity in the 450-500- cm^{-1} region. Pyrazine is expected to show one absorption in this range, and assignment of these bands is difficult. However, both bands are well above the range observed for S-bonded thiocyanate. The band at 493 cm^{-1} is tentatively assigned to the ν_2 anion mode.

To summarize these infrared data for $\text{Fe}(\text{pyz})_2(\text{NCS})_2$, the pyrazine groups retain the D_{2h} symmetry of the free ligand by functioning as bidentate bridging ligands. This results in a layered polymeric structure **1**, as found by X-ray crystallography for $\text{Co}(\text{pyz})_2\text{Cl}_2$,¹ with monodentate thiocyanato-*N* anions above and below the poly- $\text{Fe}(\text{pyz})_2$ plane completing the pseudooctahedral coordination sphere around the iron(II) center.

Turning now to the question of anion bonding in $\text{Fe}(\text{pyz})_2(\text{NCO})_2$, previous research^{38,39,43,44} on the nature of NCO^- co-



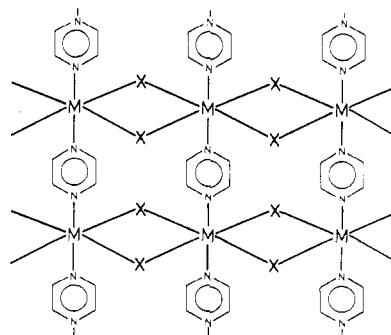
1

ordination suggests several possibilities including terminal bonding through either nitrogen or oxygen and bridging, either as $\text{M}-\text{NCO}-\text{M}'$ or $\text{M}-\text{N}-\text{M}'$. Infrared criteria have been established for determining some of these coordination modes.^{38,39,43}

The three normal vibrational modes of the linear NCO^- anion are the asymmetric stretching vibration ν_1 (ν_{CN}), the bending mode ν_2 (δ_{NCO}), and the pseudosymmetric stretching vibration ν_3 (ν_{CO}). In cyanate compounds these modes are appreciably mixed. From the infrared spectrum of KNCO ⁴⁵ the following assignments (cm^{-1}) have been made for the free anion: ν_1 2170; ν_2 629; ν_3 1254. The value of ν_3 was calculated from the Fermi resonance interaction.⁴⁶ From the infrared spectrum of $\text{Fe}(\text{pyz})(\text{NCO})_2$ (Figure S1) we can make the following assignment (cm^{-1}): ν_1 2200 s, 2100 sh; ν_2 658 s, 620 s. The ν_1 and ν_2 modes both appear to be split, and ν_3 was not observed. It has been noted previously^{38,39,43} that upon coordination the frequency of ν_1 is increased compared to the free-ion value. For $\text{Fe}(\text{pyz})(\text{NCO})_2$, the value of 2200 cm^{-1} falls within the range for either a terminally N-bonded or bridging NCO^- anion, and this absorption is not useful in distinguishing these two coordination modes.

The magnitude of the splitting of ν_2 has been found to be a good indicator for the presence of bridging NCO^- anions.^{38,39,43} In terminally N-bonded cyanate complexes this band is often split, but usually by only a few wavenumbers. The ν_2 splitting of 38 cm^{-1} in $\text{Fe}(\text{pyz})(\text{NCO})_2$ indicates a bridging mode for the anion. The $>\text{NCO}$ mode of bridging has been demonstrated by X-ray crystallography in AgNCO ,⁴⁷ where the ν_2 vibration is split by 59 cm^{-1} ,⁴³ and is the most common bridging mode for the cyanate ion. It seems likely that this mode of anion bridging is present in the iron complex. The failure to observe the ν_3 anion vibration in $\text{Fe}(\text{pyz})(\text{NCO})_2$ is not unexpected since in other complexes containing bridging cyanate groups this band is often of very low intensity.³⁹

Including the pyrazine vibrations discussed above, the infrared data are consistent with either the cross-linked linear chain structure **2** ($\text{X} = \text{NCO}$) or the cross-linked layer structure **3**.



2

Mössbauer spectra in the magnetically ordered state (vide infra)

(36) Goldstein, M.; Unsworth, W. D. *Spectrochim. Acta, Part A* **1971**, *27A*, 1055.

(37) Lewis, J.; Nyholm, R. S.; Smith, P. W. *J. Chem. Soc.* **1961**, 4591.

(38) Sabatini, A.; Bertini, I. *Inorg. Chem.* **1965**, *4*, 959.

(39) Bailey, R. A.; Kozak, S. L.; Michelson, T. W.; Mills, W. N. *Coord. Chem. Rev.* **1971**, *6*, 407.

(40) Clark, R. J. H.; Williams, C. S. *Spectrochim. Acta* **1966**, *22*, 1081.

(41) Kinell, P. O.; Strandberg, B. *Acta Chem. Scand.* **1959**, *13*, 1607.

(42) Little, B. F.; Long, G. *J. Inorg. Chem.* **1978**, *17*, 3401 and references therein.

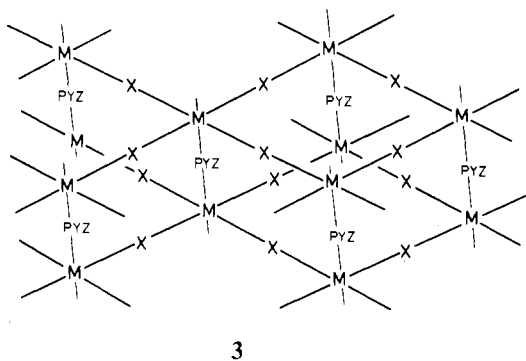
(43) Nelson, J.; Nelson, S. M. *J. Chem. Soc. A* **1969**, 1597.

(44) Forster, D.; Goodgame, D. M. L. *J. Chem. Soc.* **1965**, 1286.

(45) Maki, A. A.; Decius, J. C. *J. Chem. Phys.* **1959**, *31*, 772.

(46) Decius, J. C.; Gordon, J. J. *J. Chem. Phys.* **1967**, *47*, 1286.

(47) Britton, D.; Dunitz, J. D. *Acta Crystallogr.* **1965**, *18*, 424.



allow us to rule out **3** as a possible structure.

Electronic Spectra. Both complexes exhibit broad absorption bands in the near-infrared region (4000–15000 cm^{-1}), with band splitting being observed in the case of $\text{Fe}(\text{pyz})_2(\text{NCS})_2$ (Table II). These spectra are diagnostic of pseudooctahedral high-spin iron(II) complexes and arise from transitions between a ground electronic state derived from ${}^5T_{2g}$ to excited states derived from 5E_g in O_h symmetry. If the average ligand field in $\text{Fe}(\text{pyz})_2(\text{NCS})_2$ is represented by taking the average position of the two band maxima,⁴² we obtain a value of 11 500 cm^{-1} , essentially identical with that for $\text{Fe}(\text{pyz})(\text{NCO})_2$. The ligand field spectra of these complexes are very similar to those reported¹⁹ for the halide derivatives $\text{Fe}(\text{pyz})_2\text{X}_2$ ($\text{X} = \text{Cl}, \text{Br}, \text{I}$) and $\text{Fe}(\text{pyz})\text{Cl}_2$.

The intense colors of the present complexes, and of the mono- and bis(pyrazine)iron(II) halides¹⁹ are presumably a consequence of charge-transfer bands in the visible region of the spectra (Table II). Charge-transfer transitions in metal-pyrazine complexes are thought to be predominantly from the metal ion to a low-lying empty antibonding π^* orbital of the pyrazine ring.^{48,49} In contrast, the tetrakis(pyridine)iron(II) halide and thiocyanate complexes, as well as $\text{Fe}(\text{py})_2\text{Cl}_2$ and $\text{Fe}(\text{py})_2(\text{NCO})_2$, are all pale yellow.⁴² In these latter compounds the metal-to-ligand charge-transfer transitions probably occur at higher energy in the ultraviolet region. This is consistent with the better π -acceptor properties of pyrazine compared to those of pyridine.

It has been noted⁵⁰ that for complexes containing either an FeN_4X_2 or FeN_2X_4 chromophore to be intensely colored, the combined presence of pyrazine and either a halide or pseudohalide was necessary. This suggests that the halide or pseudohalide anions also play a role in the charge-transfer process. Because of the ease of oxidation of halide and pseudohalide ions, it is likely that the role of the anion in the charge-transfer process is ligand to metal, which then facilitates metal-to-pyrazine charge transfer.

Magnetic Susceptibility. Data for magnetic susceptibility and magnetic moment as a function of temperature (4.2–300 K) are given in Table S1.³⁵ Both complexes have strongly temperature-dependent moments, falling monotonically from about 5.2 μ_B at room temperature to 1.87 and 0.88 μ_B at 4.2 K for $\text{Fe}(\text{pyz})_2(\text{NCS})_2$ and $\text{Fe}(\text{pyz})(\text{NCO})_2$, respectively, and both exhibit susceptibility maxima at about 8 and 38 K, respectively. It is thus clear that magnetic exchange pathways are operative in both of these derivatives and that the exchange is antiferromagnetic.

Magnetic susceptibility data for $\text{Fe}(\text{pyz})_2(\text{NCS})_2$ in the 80–300 K temperature range were reported by Figgis et al.²⁷ some years ago. Agreement between the earlier data and those obtained in the present study is poor. The data reported here were recorded over the temperature range 4.2–300 K on two separate occasions by using two independently prepared samples of $\text{Fe}(\text{pyz})_2(\text{NCS})_2$, and agreement between the two sets of data was excellent. In the earlier study²⁷ neither the method of preparation nor any spectroscopic data were reported, so it is pointless to speculate on the reason for the poor agreement.

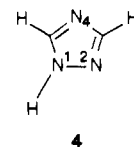
The magnetic properties of $\text{Fe}(\text{pyz})_2(\text{NCS})_2$ reported here are quite different from those of the monomeric⁵¹ $\text{Fe}(\text{py})_4(\text{NCS})_2$,

Table II. Electronic Spectra of the Complexes

compd	abs max, cm^{-1}		
$\text{Fe}(\text{pyz})_2(\text{NCS})_2$	19 400	12 900	10 200
$\text{Fe}(\text{pyz})(\text{NCO})_2$	16 000	11 200	

which has a temperature-independent moment of 5.5 μ_B between 90 and 295 K.⁵² There are, however, several other thiocyanate complexes of iron(II) that exhibit interesting magnetic phenomena. For example, $\text{Fe}(\text{py})_2(\text{NCS})_2$ undergoes a metamagnetic transition at approximately 6 K to a one-dimensional ferromagnetically ordered state,^{53–55} and the susceptibility vs. temperature curve of $\text{Fe}(\text{bpy})(\text{NCS})_2$ ($\text{bpy} = 2,2'$ -bipyridine) shows a maximum at about 18 K.⁵⁶ In both of the latter cases, however, the magnetic exchange interactions proceed via bridging thiocyanate networks, while in $\text{Fe}(\text{pyz})_2(\text{NCS})_2$ it is the neutral ligands that bridge the metal ions and propagate the superexchange.

More directly comparable to $\text{Fe}(\text{pyz})_2(\text{NCS})_2$ is $\text{Fe}(\text{trz})_2(\text{NCS})_2$ ($\text{trz} = 1,2,4$ -triazole, **4**). X-ray powder photographs⁵⁷ have shown



the triazole complex to be isomorphous with $\text{Co}(\text{trz})_2(\text{NCS})_2$,⁵⁸ which exists as a two-dimensional sheetlike polymer, formed by the triazole ligand using nitrogen atoms N(2) and N(4) to bridge adjacent centers. The thiocyanate groups are N-bonded in axial positions to complete the pseudooctahedral coordination. This is entirely analogous to structure **1** proposed for $\text{Fe}(\text{pyz})_2(\text{NCS})_2$. For the triazole compound, powder susceptibility data⁵⁷ reveal a maximum at a temperature of 8.8 K, while single-crystal measurements⁵⁹ show a maximum in $\chi_M(T)$ at 12.2 K. In $\text{Fe}(\text{pyz})_2(\text{NCS})_2$ we find $T(\chi_{\text{max}}) \approx 8$ K, suggesting that, at least in these complexes, pyrazine and 1,2,4-triazole are roughly comparable in propagating exchange interactions.

As suggested by the proposed structure **1**, we have analyzed the $\chi_M(T)$ data for $\text{Fe}(\text{pyz})_2(\text{NCS})_2$ using Lines' high-temperature series expansion for a two-dimensional square-planar antiferromagnet in the Heisenberg limit.⁶⁰ A least-squares procedure allowed both J and g to vary so as to minimize the function F :

$$F = \left[\frac{1}{n} \sum_i \left(\frac{\chi_i^{\text{calcd}} - \chi_i^{\text{obsd}}}{\chi_i^{\text{obsd}}} \right)^2 \right]^{1/2} \quad (1)$$

where n is the number of data points. The best fit was obtained with $J = -0.44 \text{ cm}^{-1}$ and $g = 2.21$ ($F = 0.0655$), and the calculated and experimental curves are shown in Figure 1. There is considerable disparity between the two in the vicinity of the susceptibility maximum, and the parameters obtained from the fit are, at best, semiquantitative and should be viewed with caution. The discrepancies may be attributed to inadequacies in the model as applied to an $S = 2$ system. It is not usually possible to represent the magnetic properties of high-spin iron(II) complexes

(48) Lever, A. B. P. *J. Chem. Educ.* **1974**, *51*, 612.

(49) Lever, A. B. P.; Lewis, J.; Nyholm, R. S. *J. Chem. Soc.* **1964**, 4761.

(50) Haynes, J. S. Ph.D. Thesis, University of British Columbia, 1985.

(51) Sötofte, I.; Rasmussen, S. E. *Acta Chem. Scand.* **1967**, *21*, 2028.

(52) Gerloch, M.; McMeekin, R. F.; White, A. M. *J. Chem. Soc., Dalton Trans.* **1975**, 2452.

(53) Reiff, W. M.; Frankel, R. B.; Little, B. F.; Long, G. J. *Inorg. Chem.* **1974**, *13*, 2153.

(54) Foner, S.; Frankel, R. B.; Reiff, W. M.; Little, B. F.; Long, G. J. *Solid State Commun.* **1975**, *16*, 159.

(55) Foner, S.; Frankel, R. B.; Reiff, W. M.; McNiff, E. J.; Little, B. F.; Long, G. J. *AIP Conf. Proc.* **1975**, *No. 24*, 363.

(56) Dockum, B. W.; Reiff, W. M. *Inorg. Chem.* **1982**, *21*, 391, 1406.

(57) Haasnoot, J. G.; Groeneveld, W. L. *Z. Naturforsch., B: Anorg. Chem., Org. Chem.* **1977**, *32B*, 553.

(58) Engelfriet, D. W.; den Briken, W.; Verschoor, G. C.; Gorter, S. *Acta Crystallogr., Sect. B: Struct. Crystallogr. Cryst. Chem.* **1979**, *B35*, 2922.

(59) Engelfriet, D. W.; Groeneveld, W. L.; Nap, G. M. *Z. Naturforsch., A: Phys., Phys. Chem. Kosmophys.* **1980**, *35A*, 852.

(60) Lines, M. E. *J. Phys. Chem. Solids* **1970**, *31*, 101.

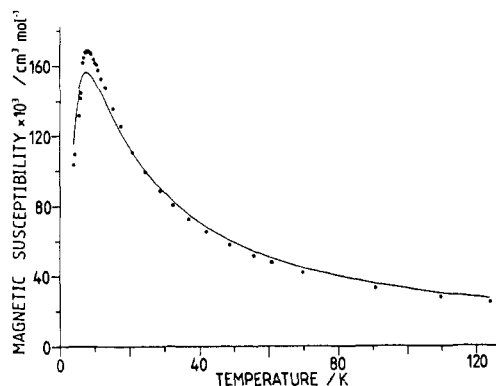


Figure 1. Temperature dependence of the magnetic susceptibility for $\text{Fe}(\text{pyz})_2(\text{NCS})_2$. The solid line was generated from the two-dimensional Heisenberg model of ref 60, with $J = -0.44 \text{ cm}^{-1}$ and $g = 2.21$.

accurately by using either a pure isotropic (Heisenberg) or anisotropic (Ising) model (and there is no solution available for a two-dimensional Ising model applicable to spin $S = 2$). In addition, the model neglects zero-field-splitting effects and also ignores any extended three-dimensional order. In fact, it has been pointed out that Lines' model is not of quantitative value below the ordering temperature;⁶⁰ accordingly, calculations were also done by employing the high-temperature data only ($T > 8.0 \text{ K}$). An excellent fit to these data was obtained with $J = -0.36 \text{ cm}^{-1}$ and $g = 2.12$ ($F = 0.0112$).

For $\text{Fe}(\text{pyz})(\text{NCO})_2$ the susceptibility maximum is at approximately 38 K, indicating substantially stronger magnetic interactions in this case. Spectroscopic data show both bridging pyrazine and bridging cyanate anions, and it is likely that both types of bridging groups contribute to some extent to the superexchange between metal centers. The presence of such a complex bridging network renders analysis of the susceptibility data more difficult. The exchange mechanisms are expected to be different through the pyrazine π system and through the (probable) $>\text{NCO}$ bridge. In the extreme case where one path is dominant, the susceptibility may be represented by a one-dimensional linear-chain model. At the other extreme where exchange coupling proceeds equally through both bridging ligands, a two-dimensional model is more appropriate.

We have therefore analyzed the magnetic data for $\text{Fe}(\text{pyz})(\text{NCO})_2$ via both a linear-chain model and a two-dimensional model, for $S = 2$ in the Heisenberg limit. Within this limit there are two theoretical approximations for an antiferromagnetic linear chain that may be applied to $S = 2$. Wagner and Friedberg⁶¹ have scaled the exact results of Fisher⁶² to the series expansion results of Rushbrooke and Wood⁶³ to obtain an expression for the temperature dependence of χ_M . The other approximation method is an interpolation scheme developed by Weng,⁶⁴ and we have used the coefficients generated by Hiller et al.⁶⁵ to reproduce Weng's numerical results.

Both linear-chain models produce similarly shaped curves with rather flat maxima. With the ranges of J and g values used, the computed curves never gave a satisfactory match to the experimental data for $\text{Fe}(\text{pyz})(\text{NCO})_2$ over the entire temperature range. Employing only the experimental data above the ordering temperature ($T > 27 \text{ K}$) and the Weng model, we obtained an excellent fit to the high-temperature data with $J = -5.18 \text{ cm}^{-1}$ and $g = 2.28$ ($F = 0.0037$). These parameters were used to generate the solid line in Figure 2a. Lines' two-dimensional model discussed above also produced a good fit to the high-temperature data with $J = -2.12 \text{ cm}^{-1}$ and $g = 2.31$ ($F = 0.0048$). The solid line in Figure 2b was generated by using these parameter values.

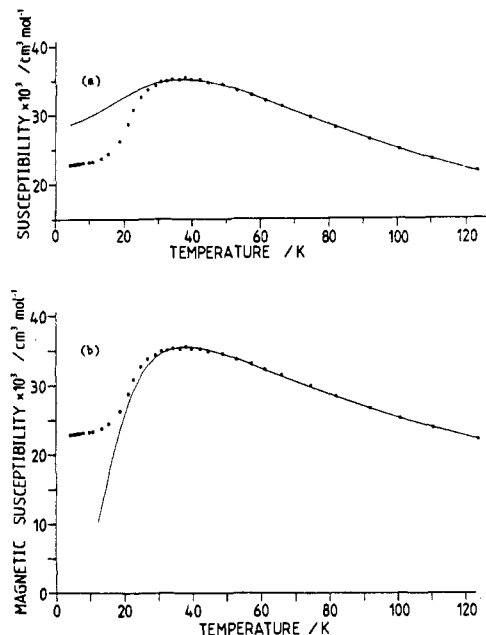


Figure 2. Temperature dependence of the magnetic susceptibility for $\text{Fe}(\text{pyz})(\text{NCO})_2$. In (a) the solid line was generated from the linear-chain model of ref 64, with $J = -5.18 \text{ cm}^{-1}$ and $g = 2.28$. The solid line in (b) is based on the 2D Heisenberg model,⁶⁰ with $J = -2.12 \text{ cm}^{-1}$, $g = 2.31$.

The differences between the 1D and 2D theoretical predictions in Figure 2 are very suggestive.⁶⁶ Both models fit the experimental susceptibility data quite well on the high-temperature side of the maximum, but they fall in opposite senses on the low-temperature side, where the antiferromagnetic exchange interactions are most strongly manifested. This suggests that the true situation in $\text{Fe}(\text{pyz})(\text{NCO})_2$ corresponds to something intermediate between the 1D and 2D Heisenberg models. Indeed, Mössbauer data discussed below show that the magnetic interactions are of a highly anisotropic 2D character (2D Ising-like), in agreement with this idea. It appears that some sort of averaging of the two theoretical curves in Figure 2 should be able to reproduce the experimental data quite closely. However, as there is no independent way of assessing what weighting factors to use in such an averaging process, we have not pursued this idea further.

Comparison of our results for $\text{Fe}(\text{pyz})(\text{NCO})_2$ with those for $\text{Fe}(\text{py})_2(\text{NCO})_2$ ⁴² is of interest, as both complexes are thought to contain $>\text{NCO}$ ligands that use a one-atom bridge to link the metal centers. This results in a linear-chain structure for the pyridine complex and a cross-linked linear chain in the pyrazine derivative. Despite this structural similarity, the magnetic properties of the complexes are strikingly different. $\text{Fe}(\text{pyz})_2(\text{NCO})_2$ orders antiferromagnetically, whereas $\text{Fe}(\text{py})_2(\text{NCO})_2$ is ferromagnetic.⁴² The lack of X-ray structural data for both complexes makes it difficult to explain this difference in magnetic properties, although the following rationale seems reasonable. Since $\text{Fe}(\text{py})_2(\text{NCO})_2$ is ferromagnetic, the orbital overlap through the nitrogen atom of the bridging cyanate group must be orthogonal. A similar *intra-chain* ferromagnetic interaction might be expected in $\text{Fe}(\text{pyz})(\text{NCO})_2$. The chains in the pyridine derivative are effectively isolated, whereas in the pyrazine complex they are linked by pyrazine bridges. The π system of pyrazine is likely to present an *interchain* antiferromagnetic exchange pathway, and if neighboring ferromagnetic chains are coupled antiferromagnetically, a net antiferromagnetic interaction would result.

⁵⁷**Fe Mössbauer Spectra.** At 293 and 78 K both complexes show simple quadruple-split Mössbauer spectra, with isomer shift and quadrupole splitting values (Table III) typical of pseudooctahedral high-spin iron(II) compounds. The isomer shifts are very similar

(61) Wagner, G. R.; Friedberg, S. A. *Phys. Lett.* **1964**, *9*, 11.

(62) Fisher, M. E. *Am. J. Phys.* **1964**, *32*, 343.

(63) Rushbrooke, G. S.; Wood, P. S. *Mol. Phys.* **1958**, *1*, 257.

(64) Weng, C. H. Ph.D. Thesis, Carnegie-Mellon University, 1968.

(65) Hiller, W.; Strahle, J.; Datz, A.; Hanack, M.; Hatfield, W. E.; Gütlich, P. *J. Am. Chem. Soc.* **1984**, *106*, 329.

(66) Papaefthymiou, V., personal communication.

Table III. Mössbauer Parameters of the Complexes

compd	T, K	δ , ^a mm s ⁻¹	ΔE_Q , mm s ⁻¹	Γ , mm s ⁻¹	ref ^b
Fe(py ₂) ₂ (NCS) ₂	293	1.01	2.45	0.32	
	78	1.11	2.63	0.34	
Fe(py ₂)(NCO) ₂	293	1.05	2.04	0.35	
	78	1.17	2.75	0.43	
Fe(py) ₄ (NCS) ₄	RT ^c	1.05	1.54	0.25	42
	78	1.17	2.01	0.26	
Fe(py ₂) ₂ (NCO) ₂	RT	1.09	1.54	0.42	42
	78	1.21	2.16	0.42	

^a Relative to metallic iron at room temperature. ^b This work, unless otherwise noted. ^c Room temperature.

to those reported⁴² for Fe(py)₄(NCS)₂ and Fe(py)₂(NCO)₂, presumably a consequence of the identical FeN₄N'₂ chromophores in all four complexes. On the other hand, the quadrupole splittings of the pyrazine derivatives are substantially greater than those of the pyridine complexes, indicating larger pseudotetragonal distortions in the present compounds. The large quadrupole splittings in Fe(py₂)₂(NCS)₂ and Fe(py₂)(NCO)₂ are diagnostic of orbitally nondegenerate ground states,^{67,68} and as we shall see below the ground state in both cases is ⁵B_{2g}, the same as in the two pyridine complexes.

In view of the susceptibility maxima observed for the pyrazine derivatives, detailed low-temperature Mössbauer measurements were made in order to study the onset of magnetic ordering. For Fe(py₂)₂(NCS)₂ spectra were recorded in the range 1.8–12 K, and for Fe(py₂)(NCO)₂ in the range 4.2–40 K.

At 9.8 K the Mössbauer spectrum of Fe(py₂)₂(NCS)₂ remains a symmetric quadrupole doublet with narrow lines. At slightly lower temperatures the doublet begins to broaden asymmetrically and magnetic hyperfine structure is apparent at 9.1 K. At 8.4 K we observe a fully magnetically split spectrum, although with very broad lines that result from relaxation effects that are occurring within the Mössbauer frequency window ($\sim 10^7$ s⁻¹). Line broadening persists down to about 7 K, and between 7 and 9 K satisfactory simulations of the spectra could not be achieved by using a static molecular field model.³²

In a preliminary report²⁸ we tentatively assigned the Néel transition temperatures as $T_N = 9.1 \pm 0.2$ K, as this is where the onset of hyperfine structure is observed, but it now appears that this assignment is probably in error. The susceptibility maximum occurs at ~ 8 K, and as the critical point should correspond to the point of maximum slope on a χ_M vs. T plot, it is clear from Figure 1 that this must occur on the low-temperature side of the maximum. In fact, it is quite usual in low-dimensional magnetic systems to find T_N significantly below $T(\chi_{max})$.⁶⁹ However, our inability to simulate the spectra in the 7–9 K region precludes an accurate determination of the Néel point at this time.

The line broadening observed in this temperature range may arise either from slow single-ion relaxation effects or from soliton (domain wall) dynamics.^{70,71} We are undertaking detailed analysis of the spectra using methods outlined by de Jongh et al.,⁷² as well as some experiments on samples of Fe_{1-x}Zn_x(pyz)₂(NCS)₂. This work should enable us to distinguish between single-ion and soliton effects and to determine the critical point precisely.

Below 7 K the lines are narrow again and the Mössbauer spectra of Fe(py₂)₂(NCS)₂ are accurately reproduced by a static molecular field model based on the results of Künig.³² In this method the parameters employed to calculate a theoretical spectrum are the isomer shift δ , the line width Γ , the magnitude and sign of the quadrupole coupling constant e^2qQ , the asymmetry parameter η

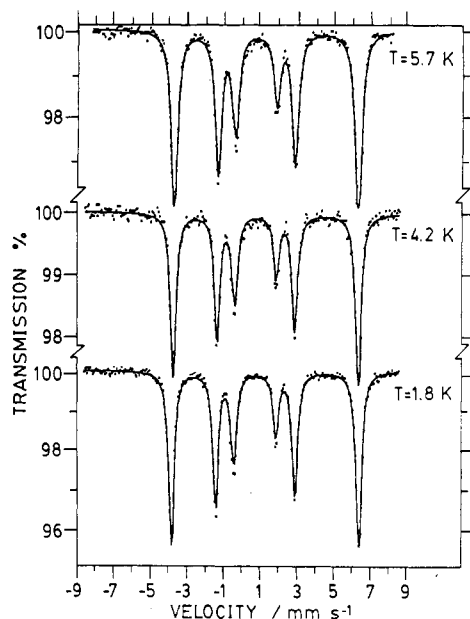


Figure 3. Mössbauer spectra of Fe(py₂)₂(NCS)₂ in the antiferromagnetically ordered regime. The simulations are based on the hyperfine parameters given in Table IV.

Table IV. Hyperfine Parameters Determined from Simulations of Mössbauer Spectra below T_N

param	Fe(py ₂) ₂ (NCS) ₂	Fe(py ₂)(NCO) ₂
δ , mm s ⁻¹	1.14 ± 0.01	1.17 ± 0.01
ΔE_Q , mm s ⁻¹	+2.71 ± 0.05	+2.78 ± 0.03
η	0.00 ± 0.05	0.47 ± 0.01
θ , deg	40.9 ± 0.2	92.0 ± 0.3
ϕ , deg		90 ± 2
H_{eff} , T	27.8 ± 0.1 ^a	18.0 ± 0.01 ^b

^a At 1.80 K. ^b At 4.20 K.

of the electric field gradient (EFG), the effective magnetic field at the nucleus H_{eff} , and the polar angles θ and ϕ that specify the direction of the hf field with respect to the EFG axis system. Some representative spectra are shown in Figure 3, where the solid lines were computed from the parameters given in Table IV and appropriate values of H_{eff} . These results provide strong support for the proposed structure 1 of Fe(py₂)₂(NCS)₂.

The EFG is effectively axial, with its principal component V_{zz} coincident with the N(anion)–Fe–N(anion) axis, i.e., normal to the poly-Fe(py₂)₂²⁺ sheets. The positive e^2qQ indicates a tetragonal compression of the FeN₄N'₂ chromophore, with the Fe–N(anion) distance somewhat shorter than the Fe–N(py₂) distance, and a nondegenerate ⁵B_{2g} ground state ($|xy\rangle$ orbital lowest in energy). Because of the axial symmetry, all orientations of the hf field with respect to the xy plane are equally probable and hence the angle ϕ is indeterminate. The angle θ is found to be 41°, showing that the internal field is tipped significantly out of the xy plane, whereas for structure 1 one might expect $\theta = 90^\circ$. The observed angle may result from a canting of the pyrazine rings out of the xy plane so as to maximize overlap between the appropriate iron d orbitals and the pyrazine π system for propagation of the magnetic exchange. Alternatively, it may be that the single-ion anisotropy tends to favor the spins along the z direction, and the exchange interactions through pyrazine are not sufficiently strong to align them in the xy plane. It does not seem possible to resolve this question in the absence of an X-ray structure determination.

The saturation value of the hf field at the iron nucleus in Fe(py₂)₂(NCS)₂ is approximately 28 T. For high-spin iron(II) the Fermi contact term is expected to be about 55 T, but this will be reduced by covalency, by the anisotropy, and by the opposing orbital and dipolar contributions. The orbital term should be relatively small in view of the near spin-only moment at high temperatures and the nondegenerate ground state. On the other

(67) Sams, J. R.; Tsin, T. B. *Inorg. Chem.* **1975**, *14*, 1573.

(68) Haynes, J. S.; Hume, A. R.; Sams, J. R.; Thompson, R. C. *Chem. Phys.* **1983**, *78*, 127.

(69) de Jongh, L. J.; Miedema, A. R. *Adv. Phys.* **1974**, *23*, 1.

(70) de Groot, H. J. M.; de Jongh, L. J.; Thiel, R. C.; Reedijk, J. *Phys. Rev. B* **1984**, *30*, 4041.

(71) Smit, H. H. A.; de Groot, H. J. M.; Thiel, R. C.; de Jongh, L. J.; Johnson, C. E.; Thomas, M. F. *Solid State Commun.* **1985**, *53*, 573.

(72) de Jongh, L. J.; de Groot, H. J. M.; ElMassalami, M.; Smit, H. H. A.; Thiel, R. C. *Proc. Int. Conf. Appl. Mössbauer Eff.* **1985**, paper INV-9.

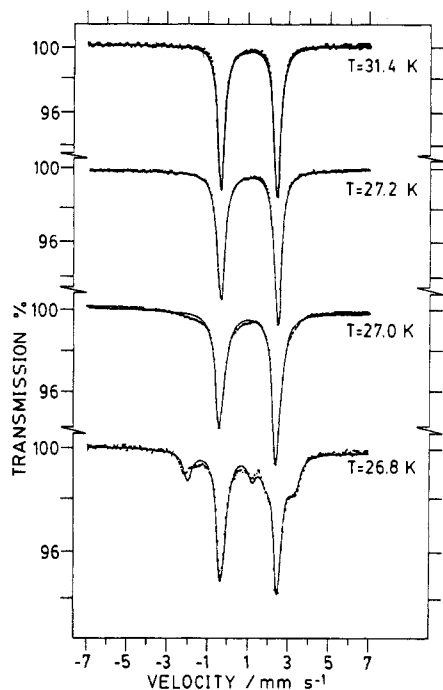


Figure 4. Mössbauer spectra of $\text{Fe}(\text{pyiz})(\text{NCO})_2$ near the Néel transition. For a discussion of the simulated spectra, see the text.

hand, the dipolar contribution, which is proportional to V_{zz} , is probably significant here. When covalency is also considered, the observed value of $H_{\text{eff}} = 28$ T seems very reasonable.

Mössbauer spectra of $\text{Fe}(\text{pyiz})(\text{NCO})_2$ are essentially independent of temperature between 78 and about 31 K. There is a slight temperature-independent asymmetry in the intensities (but not widths) of the two lines of the quadrupole doublet at 78 K, which persists down to 31.4 K and which we attribute to a texture effect. Below 31 K the spectrum becomes more asymmetric, the low-velocity line broadening more than the high-velocity one (Figure 4), probably as a result of residual short-range correlations between metal centers. (Note that this is at a temperature well

Table V. Temperature Dependence of the Hyperfine Field and Area Ratio for $\text{Fe}(\text{pyiz})(\text{NCO})_2$

T , K	H_{eff} , T	$A_{\text{afm}}/A_{\text{tot}}^a$	T , K	H_{eff} , T	$A_{\text{afm}}/A_{\text{tot}}^a$
4.2	17.9	1.000	25.4	14.7	0.657
18.2	17.5	1.000	25.8	14.3	0.595
22.4	16.7	0.952	26.2	13.8	0.522
23.5	16.2	0.893	26.6	12.7	0.399
24.4	15.7	0.813	26.8	11.2	0.306
25.0	15.1	0.722	27.0	6.8	0.163

^a Fraction of the total spectral area contributed by the antiferromagnetic phase.

below the susceptibility maximum.) In this case, however, there is no gross broadening such as that observed for the thiocyanate complex, and there is no difficulty in identifying the Néel temperature at $T_N = 27.05 \pm 0.05$ K.

Between T_N and 22.4 K the Mössbauer spectra consist of two components, a magnetic hfs pattern and a quadrupole doublet arising from a superparamagnetic (SPM) phase. As can be seen in Figure 5, the contribution of the SPM component (most evident in the line at $\sim +2.5$ mm s^{-1}) gradually decreases as the temperature is lowered, and below 22 K only the hfs pattern is detected. This critical SPM behavior may be due to the presence of a fairly broad distribution of domain sizes resulting from the very rapid precipitation of the complex from solution.

All the Mössbauer spectra of $\text{Fe}(\text{pyiz})(\text{NCO})_2$ at $T \leq 27.0$ K were well simulated with the parameters quoted in Table IV and the hf fields and SPM fractions in Table V. These simulations were found to be very sensitive to the angles θ and ϕ and to the asymmetry parameter η . The parameters in Table V allow one to rule out 3 as a possible structure of the complex. As is the case with 1, structure 3 would give an axially symmetric EFG ($\eta = 0$), and the angle ϕ would be indeterminate. On the basis of structure 2, however, an entirely plausible interpretation of the parameters can be given.

The much higher T_N found for $\text{Fe}(\text{pyiz})(\text{NCO})_2$ than that of $\text{Fe}(\text{pyiz})_2(\text{NCS})_2$ (≤ 8 K) indicates that exchange interaction through the $>\text{NCO}$ bridges is considerably stronger than that through the pyrazine rings. The simulations require that $\theta \approx \phi \approx 90^\circ$, so that H_{eff} is essentially parallel to V_{yy} . Accordingly, we

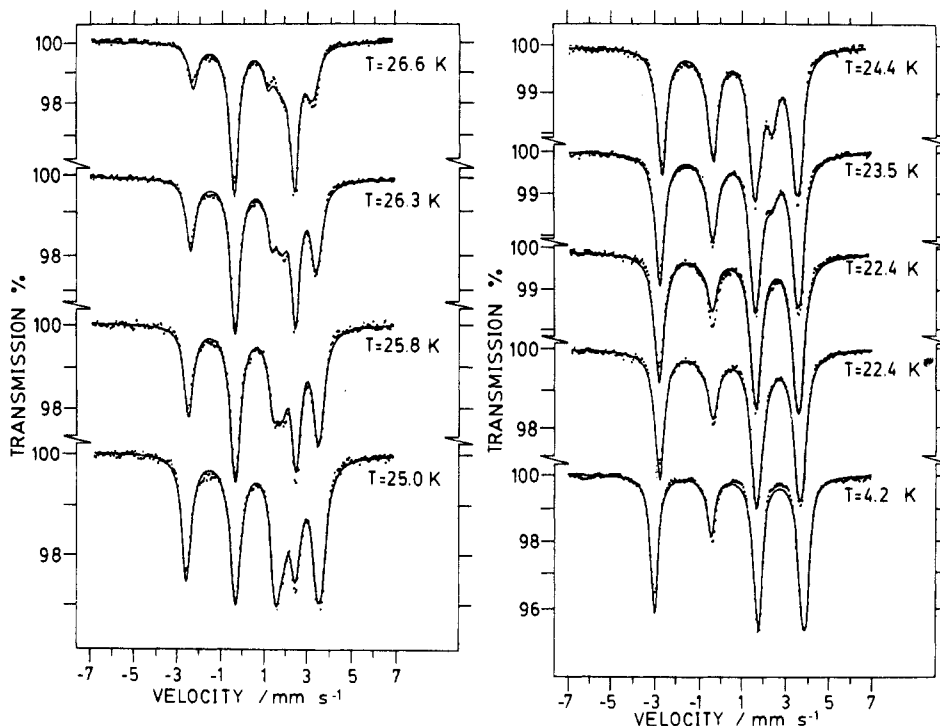


Figure 5. Mössbauer spectra of $\text{Fe}(\text{pyiz})(\text{NCO})_2$ below the Néel point. The simulations employed the parameters given in Tables IV and V. For the spectrum at 22.4 K, the upper simulation assumes only an antiferromagnetic phase, while the lower one includes a small superparamagnetic contribution. Both components are included in all spectra at $T > 22.4$ K.

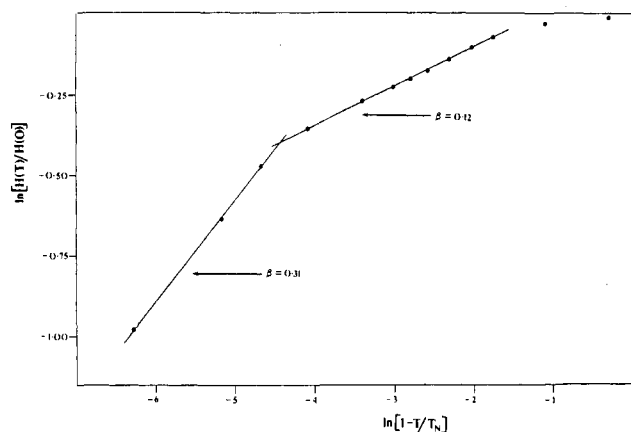


Figure 6. Double logarithmic plot of the hf field of $\text{Fe}(\text{pyz})(\text{NCO})_2$ as a function of reduced temperature in the critical region. The straight lines were constructed by linear regression and give the critical exponents indicated in the figure.

take H_{eff} and the y axis of the EFG to be along the linear-chain direction in **2**. Although the EFG z axis might be taken either parallel to the pyz-Fe-pyz direction or normal to the sheets of cross-linked linear chains, the latter choice seems the more reasonable. Since $e^2qQ > 0$ and $\eta = 0.47$, an axially compressed structure with inequivalent x and y directions is required. Such a structure would result if, as expected, the $\text{Fe-N}(\text{anion})$ bonds were shorter than the $\text{Fe-N}(\text{pyz})$ bonds and the x axis of the EFG lies along the pyz-Fe-pyz direction.

The hf field data in Table V indicate that H_{eff} saturates rapidly below T_N , much more rapidly than a Brillouin function.²⁸ This temperature dependence provides additional support for the low-dimensional nature of this system. In the critical region the sublattice magnetization, $M(T)$, is given by⁶⁹

$$M(T)/M(0) = B(1 - T/T_N)^\beta \quad (2)$$

where $M(0)$ is the saturation magnetization, B the amplitude of the singularity, and β the critical exponent. With the usual assumption that the hf field is proportional to the magnetization, a plot of $\ln [H(T)/H(0)]$ vs. $\ln (1 - T/T_N)$ should yield a straight line whose slope is β . For 3D lattices β is about $1/3$, whereas the 2D Ising model gives $\beta = 1/8$.⁷³ (A 2D Heisenberg system cannot support spontaneous magnetization at a finite temperature.) It was therefore of interest to evaluate β from the data in Table V. In the range $0.8 \leq T/T_N \leq 0.98$ we find $\beta = 0.12$ and $B = 1.14$, although closer to T_N there is an apparent change in the slope and $\beta \approx 0.3$ (see Figure 6). Such crossover in the value of the critical exponent has been reported previously in K_2MnF_4 ⁷⁴ and Rb_2FeF_4 ,⁷⁵ and there are at least two possible explanations of this behavior.

In $\text{Fe}(\text{pyz})(\text{NCO})_2$ there are in fact three possible magnetic interaction pathways: the intrachain coupling J via the $>\text{NCO}$ bridges; the interchain coupling J' through the pyrazine π system; and an interlayer interaction J'' between the sheets. From the fact that the hf field lies along a particular direction (V_{yy}), we conclude that $|J| \gg |J'|$, so that the magnetic structure within the layers is 2D Ising-like. For the sake of the present argument we can therefore ignore J' and think of J as an intralayer coupling constant. The observation of long-range 3D ordering in the Mössbauer spectra shows that $J'' \neq 0$, but as T_N is well below $T(\chi_{\text{max}})$, it is clear that $|J''| \ll |J|$. In such a case, as de Jongh

and Miedema have discussed,⁶⁹ the temperature dependence of the spontaneous magnetization over a considerable range of temperature should be that of a 2D Ising system, except very near the critical point where the influence of J'' will become apparent, since any system with $J'' \neq 0$ is ultimately 3D in character. This is in accordance with the universality hypothesis,^{76,77} which states that close enough to the critical point the value of β should be independent of the ratio $|J''/J|$, except when $J'' = 0$, where it should change discontinuously from the 3D to the 2D value. One could therefore define a crossover temperature T^* , below which the system behaves two-dimensionally with $\beta = 1/8$, whilst in the range $T_N - T^*$ the system behavior is three-dimensional with $\beta \sim 1/3$, the range $T_N - T^*$ depending on the ratio $|J''/J|$.

On the other hand, Birgenau et al.⁷⁸ have pointed out that such an apparent change in the value of β can also result from a small spread in the critical temperature, a possibility we cannot rule out in the present case. We have therefore not attempted to estimate $|J''/J|$. However, it should be mentioned that the value 1.14 for the amplitude B is close to the 2D Ising value of 1.24 but very different from the 3D Ising prediction ($B \approx 1.52$).⁶⁹ Thus, the 2D Ising characteristics of $\text{Fe}(\text{pyz})(\text{NCO})_2$ have been clearly demonstrated.

A somewhat different situation is encountered in $\text{Fe}(\text{pyz})-(\text{CF}_3\text{SO}_3)_2$, where the linear chains in **2** are formed by bidentate bridging CF_3SO_3^- ions.^{28,50} The exchange coupling is again of an antiferromagnetic nature, with a susceptibility maximum at 4.4 K, and Mössbauer spectra indicate $T_N \sim 3.8$ K. However, the intralayer anisotropy is much smaller than in the case of $\text{Fe}(\text{pyz})(\text{NCO})_2$, the susceptibility data in the range $1.9 \text{ K} \leq T \leq 120 \text{ K}$ being very well reproduced by a 2D Heisenberg model.⁵⁰ For the triflate complex it appears that exchange interactions via the pyrazine rings and those via the O-S-O bridges are of comparable magnitude.

In general, the situation regarding magnetic exchange in iron(II) complexes with bridging pyrazine ligands is by no means straightforward. Complexes of the types $\text{Fe}(\text{pyz})_2\text{X}_2$ with terminal anionic ligands and $\text{Fe}(\text{pyz})\text{X}_2$ with bridging anions as well as bridging pyrazine show a variety of magnetic properties.⁵⁰ The presence of an Fe-pyz-Fe pathway is obviously not a sufficient condition for the occurrence of significant magnetic exchange. In both types of complexes it appears that the nature of the anionic group may be playing an important role, but it does not seem possible at present to correlate the different magnetic properties with either electronic or steric features of the anions. It may be that small differences in pyrazine ring orientation can affect significantly the efficiency of exchange through this ligand, and single-crystal X-ray structural data would be invaluable in this regard.

Acknowledgment. We appreciate several interesting discussions with Dr. V. Papaefthymiou. J.S.H. thanks the UBC Graduate Scholarship Committee for scholarship awards. J.R.S. is grateful to the Ministry of Research and Technology of the Hellenic Republic for financial assistance during his sojourns at "Demokritos". Support from the Natural Sciences and Engineering Research Council of Canada is gratefully acknowledged.

Registry No. $\text{Fe}(\text{pyz})_2(\text{NCS})_2$, 109011-46-3; $\text{Fe}(\text{pyz})_2(\text{NCO})_2$, 109011-48-5.

Supplementary Material Available: Magnetic data (Table S1) and infrared spectra (Figure S1) (3 pages). Ordering information is given on any current masthead page.

(73) Fisher, M. E. *Rep. Prog. Phys.* **1967**, *30*, 615.

(74) Ikeda, H.; Hirakawa, K. *J. Phys. Soc. Jpn.* **1972**, *33*, 393.

(75) Birgenau, R. J.; Guggenheim, H. J.; Shirane, G. *Phys. Rev. B* **1970**, *1*, 2211.

(76) Griffiths, R. B. *Phys. Rev. Lett.* **1970**, *24*, 1479.

(77) Kadanoff, L. P. *Proceedings of the Fermi Summer School of Physics*; Green, M. S., Ed.; Academic: New York, 1970.

(78) Birgenau, R. J.; Guggenheim, H. J.; Shirane, G. *Phys. Rev. B* **1973**, *8*, 304.